一种零电压零电流倍流整流弧焊逆变器

陈延明[1]， 吴慧芳[1]， 曹 彪[2]， 王志强[2]
（1. 广西大学 电气工程学院，南宁 530004；2. 华南理工大学 电子学院，广州 510640）

摘 要：采用移相控制和倍流整流技术，实现零电压零电流开关全桥变换和整流二极管软开关弧焊逆变器。其中超前桥臂实现零电压开通，滞后桥臂实现零电流关断，副边整流二极管，实现零电流自然关断，整个弧焊逆变器所有的功率器件都工作在软开关状态。降低了功率器件的应力与开关损耗，降低了干扰，提高了弧焊逆变器的电磁兼容性能力，特别适合大功率场合；并且可以进一步提高开关频率，加快系统动态响应能力。文中还简单讨论了软开关范围和参数的关系。在此基础上，制作 2 kW 弧焊逆变器，结果表明，该弧焊逆变器的良好性能。

关键词：弧焊逆变器；移相控制；零电压开关；零电流开关；倍流整流
中图分类号：TM46 文献标识码：A 文章编号：0253－360X(2007)06－021－04

陈延明

0 序 言

移相全桥软开关变换电路及其派生电路，既可以实现全桥零电压开关(ZVS)，又可以实现零电压零电流开关(ZVZCS)；减小了功率器件的开关损耗与电磁干扰，改善功率器件的开关轨迹，降低功率器件的电压、电流应力，提高变换电路的性能、效率，改善电磁兼容性能力，可以提高开关频率、降低变换器的体积，提高功率密度，加快系统动态响应能力，是目前中、大功率弧焊逆变器的理想拓扑之一[1－5]。

常规的软开关弧焊逆变器，通常只考虑变压器原边功率器件软开关工作的情况，并有系列改进的方法[1－5]，但对变压器副边的整流二极管工作情况考虑不多，副边整流二极管通常工作在硬开关状态，对弧焊逆变器这种大电流输出，有时又处于空载或短路的恶劣工作状况的电源来说，其副边的开关损耗和电磁干扰很大，对弧焊逆变器的可靠性和稳定性有极大的影响，也不利于其性能的进一步提高。

为了进一步改善弧焊逆变器的软开关情形，作者在分析移相全桥零电压零电流变换电路(ZVZCS)基础上，采用倍流整流工作方式，设计大功率软开关弧焊逆变器。其中，弧焊逆变器的超前桥臂，利用变压器漏感和输出电感，实现零电压开通；利用与变压器串接的隔直电容，快速衰减电流，使得滞后桥臂可以实现零电流关断；采用低损耗的饱和电抗器，阻止电流反向振荡；副边整流二极管，工作在倍流整流方式，实现了自然换流，消除整流二极管的开关损耗，而且也避免了整流二极管反向恢复引起的振荡和尖峰[6－8]。这样，变换电路所有的功率器件都工作在软开关的条件下，进一步提高其电磁兼容性能力，提高弧焊逆变器的可靠性和稳定性。在此基础上，制作 2 kW 的弧焊逆变器，获得了比较满意的结果。

1 电路工作原理

主电路如图 1 所示，原边是移相控制的零电压零电流全桥变换电路，副边是倍流整流的工作方式。其中，全桥变换电路的功率开关 VT1 与 VT3，构成超前桥臂，功率开关 VT2 与 VT4，构成滞后桥臂；$C1$，$C3$ 和 D1～D4 分别为相应功率开关的输出电容和反并联二极管；变压器原边串接隔直电容 C_b，饱和电感 L_s，变压器有等效漏电感 L_{lk}；副边倍流整流电路，由变压器 T，两个输出等值电感 L_o1 和电感 L_o2，整流二极管 D_o1 和 D_o2 和负载构成。

详细工作模式分析如下。首先作如下假设：①电路中所有的元器件(开关管、二极管、变压器、电容、电感等)均为理想器件。② $C1=C3=C_{lead}$，$L_o1=L_o2$，n_1 为变压器原边绕组匝数，n_2 为副边绕组匝数，N 为变压器变比 n_1/n_2。③输出滤波电容足够大，在一个周期内可以使输出看作一个恒定

收稿日期：2006－07－26
基金项目：国家自然科学基金项目(50567001)；国家科技型中小企业创新基金(03C26224500661)

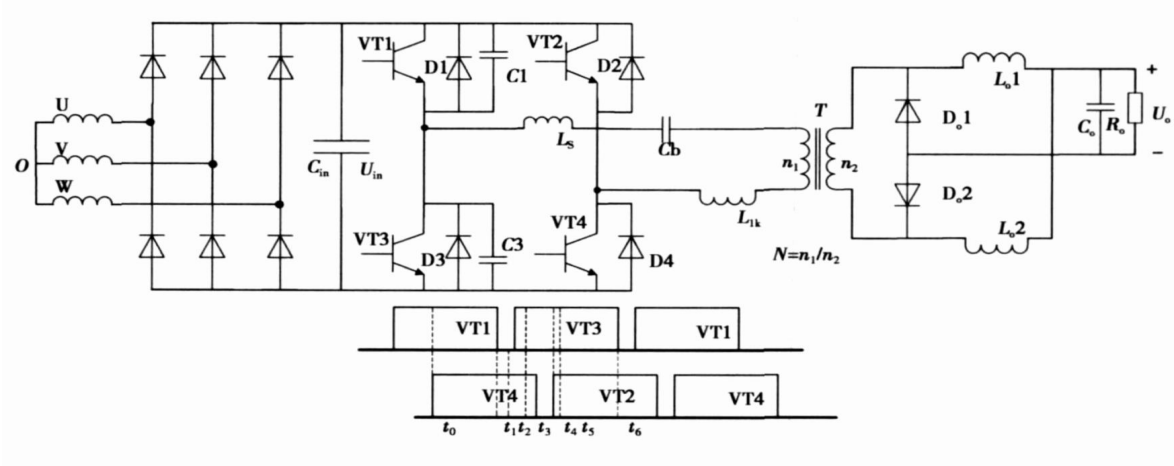

图 1 零电压零电流倍流整流变换电路

Fig. 1 ZVZCS full-bridge converter with current doubler rectifier

电压源 U_o。假定 VT1, VT3 为超前桥臂, VT2, VT4 为滞后桥臂, 其半周期内的主要工作过程, 可分为 6 个模态, 如图 2 所示, 图中有实线和虚线两种状态, 其中实线表示电流流通的路径。

1.1 开关模态 1

自初始时刻 t_0 起(图 2a), 功率开关管 VT1, VT4 均导通, 原边电压、电流方向一致, 原边向副边负载传递能量, 其负载能量由两部分提供, 一是变压器 T 传送的, 二是电感 L_o2 续流的, 副边整流二极管 D_o1 承受反压截止, D_o2 导通, 提供电流回路。原边电流 i_p 正向增大, 隔直电容 Cb 及电压 u_{Cb} 由负电压到零后正向增大, 副边滤波电感电流 i_{L_o1} 上升, 电感电流 i_{L_o2} 下降。该模态电流的方程为

$$i_{L_o1}(t)=i_{L_o1}(t_0)+\frac{\frac{U_{in}}{N}-U_o}{L_o1}(t-t_0), \tag{1}$$

$$i_{L_o2}(t)=i_{L_o2}(t_0)-\frac{U_o}{L_o2}(t-t_0), \tag{2}$$

式中: $i_{L_o1}(t_0)$, $i_{L_o2}(t_0)$ 分别为电感 L_o1 和电感 L_o2 在 t_0 时刻的电流值; U_{in} 和 U_o 分别是逆变器输入和负载输出电压; N 为变压器原边和副边的匝数比。

1.2 开关模态 2

t_1 时刻关断 VT1(图 2b), 原边电流 i_p 为 $C1$ 充电, 为 $C3$ 放电, VT1 近似零电压关断, 副边工作方式等同模态 1。i_p 为励磁电流与副边折算电流之和, 由于该模态持续时间较短, 电容 $C1$, $C3$ 电压可看作线性变化, 其方程为

$$U_{C1}=\frac{i_p}{2C_{lead}}(t-t_1), \tag{3}$$

$$U_{C3}=U_{in}-\frac{i_p}{2C_{lead}}(t-t_1)。 \tag{4}$$

到 t_2 时刻, $C1$ 两端电压升为 U_{in}, $C3$ 两端电压降为零, 功率管 VT3 的反并联二极管 D3 自然导通, 功率管 VT3 两端电压被箝位为零, 为功率管 VT3 零电压开通提供条件。

1.3 开关模态 3

t_2 时刻后开通 VT3(图 2c), 因为 D3 处于导通状态, 所以 VT3 实现零电压开通。输出电感的折算电流, 继续为隔直电容充电, 隔直电容电压 u_{Cb} 继续上升, 变压器原边电流 i_p 衰减, 变压器副边电流 i_s 同时衰减, 当 $i_s<i_{L_o1}$ 时, 由于电感电流不能突变, 故 D_o1 导通, 负担其电流差值, 变压器原、副边电压箝位为零, 原、副边不再传递能量。副边两个输出电感均进入续流阶段, 电感 L_o1 有两条续流通路, 一是通过负载, 二极管 D_o1 续流, 二是通过负载, 变压器续流, 电感 L_o2 继续通过负载, D_o2 续流, 两个电感电流均近似线性下降, 如下所示, 式中 $U_{Cb(max)}$ 是隔直电容两端的电压最大值。

$$i_p(t)=\frac{i_{L_o1}(t_2)}{N}-\frac{U_{Cb(max)}}{L_{lk}}(t-t_2), \tag{5}$$

$$i_{L_o1}(t)=i_{L_o1}(t_2)-\frac{U_o}{L_o1}(t-t_2), \tag{6}$$

$$i_{L_o2}(t)=i_{L_o2}(t_2)-\frac{U_o}{L_o2}(t-t_2)。 \tag{7}$$

1.4 开关模态 4

t_3 时刻(图 2d), 原边电流 i_p 衰减为零, 饱和电感 L_s 退出饱和状态, 电感值无限大, 阻断了反向电流, 相当于原边回路断开, 消除了电流的反向振荡, 此时, 滞后管 VT4 实现零电流关断。此后, 原边电路保持开路状态。变压器副边也没有电流, 副边电感 L_o1 和 L_o2 分别通过 D_o1 和 D_o2 续流, 为负载供电。

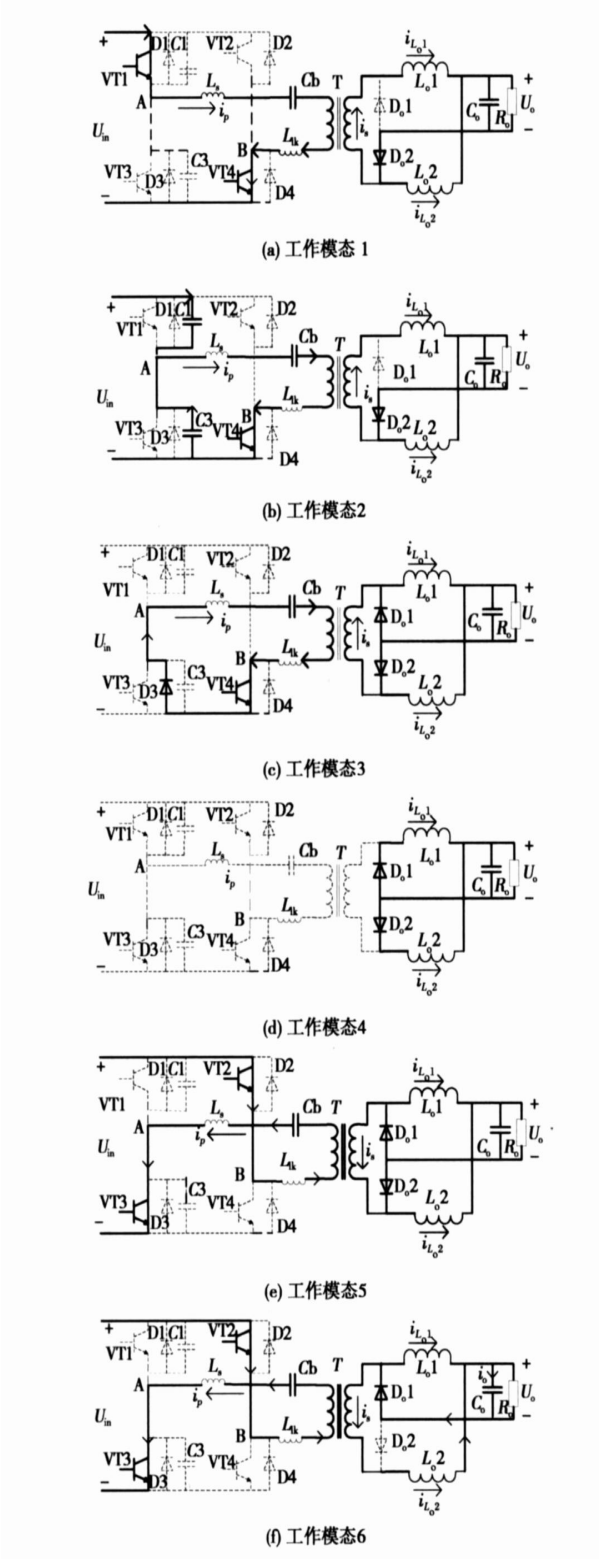

图 2　各个工作模态等效电路图

Fig 2　Equivalent circuit of each operating mode

1.5　开关模态 5

t_4 时刻开通 VT2(图 2e), 原边电流 i_p 反向线性增加, 但仍小于 i_{L_o2} 的折算值, 整流二极管电流 i_{D_o1} 上升, i_{D_o2} 下降。t_5 时刻, 变压器副边电流 i_s 等于电感 L_o2 的电流, i_{L_o2} 全部转移到 D_o1 中, D_o2 实现零电流关断, 此时, 原边电流方程为

$$i_p(t)=\frac{U_{in}+U_{Cb(max)}}{L_{lk}}(t-t_4)。\qquad(8)$$

1.6　开关模态 6

t_5 时刻后(图 2f), 电源重新向负载传递能量, 原边电流继续反向增大; 副边整流二极管 D_o1 导通、D_o2 零电流关断后, 承受反压截止。电感 L_o1 通过 D_o1 续流放电, L_o2 充电, i_{L_o1} 下降, i_{L_o2} 上升, 负半周工作工程开始, 类似于正半周。

在整个工作过程模式中, 原边全桥变换电路有向副边传送能量的过程; 有电流衰减的环流, 创造超前桥臂的零电压开通和滞后桥臂的零电流关断的条件。副边工作有变压器经一个电感向负载供电, 另一电感向负载续流供电的过程, 以及变压器不传送能量, 两个电感向负载续流供电的过程, 在两个状态转换过程中, 实现输出二极管的零电流关断, 使得整个变换电路的功率器件都可以实现软开关, 降低功率器件的开关损耗, 减少电磁干扰, 提高了系统电磁兼容性能力。

2　电路实现和试验结果

整个控制电路, 基于芯片 UC3875 芯片来设计, UC3875 有电压控制工作模式, 也有电流控制工作模式, 可以根据弧焊逆变器的外特性, 对所需要的电压调节器, 电流调节器进行灵活设计。在实际设计中, 两个输出滤波电感可以采用同一磁芯绕制, 匝数相等, 磁路相同, 保证其电感值相同; 同时, 正半周和负半周的 PWM 脉宽严格对称; 并且可以通过电流调节器设计, 保证正负半周电流对称; 根据负载的情况, 开关频率的大小, 变压器漏感大小, 选择适当的隔直电容和低损耗的饱和电抗器, 使得超前桥臂有较大的零电压开通范围, 滞后桥臂有较大的零电流关断范围, 同时副边整流二极管, 也有较大自然换流的软开关范围, 所设计的隔直电容最大电压, 只有输入电压的 1/15, 保证原边能量有效传递到副边。

图 3a 是超前管电压及电流的波形, 可以看出该开关管是零电压开通。图 3b 是滞后桥臂的一个开关管的电压波形及其电流波形, 可以看出该开关管实现了零电流关断。图 3c 是副边次级整流二极管的电压和电流的波形, 从该波形也可以看出, 次级二极管实现零电流关断, 实现了自然换流, 次级无尖峰电压。

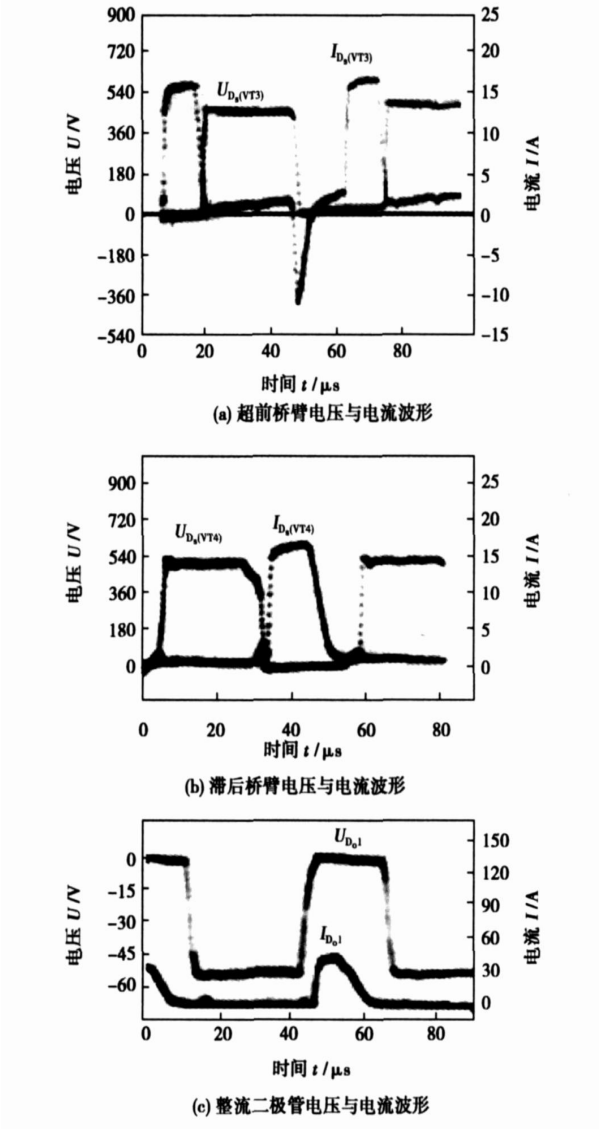

图 3 试验波形

Fig 3 Experimental results

3 结 论

研制了一种零电压零电流开关倍流整流弧焊逆变器,其超前管实现了宽范围的零电压开通,滞后管实现了宽范围的零电流关断,副边整流二极管也实现宽范围零电流关断,弧焊逆变器中的所有的功率器件均实现了软开关,降低了开关损耗,减小了开关噪声与电磁干扰,提高了开关频率与效率,改善了电磁兼容性能力,电路简单可靠实用,适合大功率应用场合,有着良好的广泛的应用前景,为弧焊逆变器稳定可靠工作提供一条新的、有效的途径。

参考文献:

[1] Cho J G, Sabatk J A, Hua G C, *et al*. Zero-voltage and zero-current-switching full bridge PWM converter for high-power applications[J]. IEEE Transactions on Power Electronics, 1996, 11(4): 622—628.

[2] 曹 彪, 陈延明, 黄石生, 等. 一种新型的软开关弧焊逆变器[J]. 焊接学报, 1998, 19(2): 110—114.

[3] 陈延明, 王志强, 曹 彪, 等. 一种新型的移相软开关变换电路[J]. 电力电子技术, 1999, 33(1): 12—14.

[4] 薛家祥, 余文松, 罗卫红. 电流模式控制的零电压软开关弧焊逆变器[J]. 焊接学报, 2002, 23(4): 35—36.

[5] Koo G B. New zero-voltage-switching phase-shift full-bridge converter with low conduction losses[J]. IEEE Transactions on Industrial Electronics, 2005, 52(1): 228—235.

[6] Kutkut N H, Divan D M, Gascoigne R W. An improved full-bridge zero-voltage switching PWM converter using a two-inductor rectifier[J]. IEEE Transactions on Industry Applications, 1995, 31(1): 119—126.

[7] 阮新波, 王建冈, 陈乾宏. 一种改进的倍流整流方式ZVS PWM全桥变换器[J]. 电工技术学报, 2002, 17(2): 71—75.

[8] Sun J. Integrated magnetics for current-doubler rectifiers[J]. IEEE Transactions on Power Electronics, 2004, 19(3): 582—590.

作者简介: 陈延明, 男, 1966 年出生, 博士, 教授。主要研究方向为电力电子拓扑、建模与控制, 弧焊逆变器。发表论文 20 篇。

Email: yanmingchen@126.com

vector; seam tracking; welding mobile robot

Simulation on equivalent stress in soldered joints of QFP devices with different leads XUE Songbai, WU Yuxiu, HAN Zongjie, HUANG Xiang (College of Materials Science and Technology, Nanjing University of Aeronautics and Astronautics, Nanjing 210016, China). p17—20

Abstract: Finite element method was used to simulate residual stress in soldered joints of QFP devices with different leads. Results indicate that the PCB is warped outward, but the distortion is small. The ceramic plate is warped upward and the distortion of its integral structure is obvious after thermal cycle. At the same time, the expending of the crack in soldered joint will be aggravated for the pull stress from ceramic plate to the lead.

The largest strain value emerges in outside of the soldered joints. The equivalent stress is relatively large in the root and toe of the soldered joint of QFP gull wing lead that the stress is larger in the root than that in the toe, but that in the middle area of the soldered joint is the least. The simulating results show that the largest stress was endured by the soldered joint of QFP with 32 leads, larger stress endured by the soldered joint of QFP with 48 leads, and the least stress endured by the QFP with 100 leads. The tensile test shows that the soldered joint of the QFP device with 100 leads possesses the biggest tensile strength than that of the QFP with 48 leads and the QFP with 32 leads, which is concordant with the numerical simulation results.

Key words: finite element method; equivalent stress; life prediction; quad flat package

A zero-voltage and zero-current welding inverter with current doubler rectifier CHEN Yanming[1], WU Huifang[1], CAO Biao[2], WANG Zhiqiang[2] (1. College of Electrical Engineering, Guangxi University, Nanning 530004, China; 2. Electric Power College, South China University of Technology, Guangzhou 510641, China). p21—24

Abstract: A full-bridge with zero-voltage and zero-current switching (ZVZCS) PWM DC-DC welding inverter by employing phase-shift and current-doubler-rectifier is presented. The zero-voltage turn-on was achieved for the leading-leg of the converter, and zero-current turn-off was achieved for the lagging-leg, and the rectifier diodes in the secondary side were turned off naturally. All the power semiconductors in the converter were operated with soft-switching condition. Hence the switching stresses, losses and interferes were reduced, and electromagnetic compatibility is improved. It is especially suitable for the high power output applications. The switching frequency can be increased, and the dynamic response can be improved. The soft-switching operating range and the design considerations were discussed. Finally, a 2 kW welding inverter was designed, and the experimental results show its the good performances.

Key words: welding inverter; phase-shift control; zero-voltage-switch; zero-current-switch; current-doubler rectifier

Modeling and simulation of weaving arc in submerged arc welding HONG Bo, HUANG Jun, PAN Jiluan, QU Yuebo* (Department of Mechanical Engineering, Xiangtan University, Xiangtan 411105, Hunan, China). p25—28

Abstract: According to the characteristics of submerged arc welding with alternative wire feed system, the seam tracking process of the submerged—arc welding was studied. The models to simulate welding power, welding arc and scaming the V groove were founded, and the general simulation model of welding system was established based on these models. The influences of groove type, welding power and forms of metal transfer on the output welding current were studied and the effects of the main parameters of arc sensor on seam deveiation and welding parameters were also analyzed. The studies offer a theoretical foundation to the establish the auto seam tracking system of weaving arc sensor in submerged arc welding.

Key words: weaving arc; seam tracking; modeling; simulation

Numerical simulation on temperature field in laser-plasma arc hybrid welding LI Zhining, CHANG Baohua, DU Dong, WANG Li (Key Laboratory for Advanced Materials Processing Technology, Tsinghua University, Beijing 100084, China). p29—33

Abstract: A three dimensional heat transfer model was put forward for the laser-plasma arc hybrid welding, which combines the mathematical models of two heat sources. The model of laser welding is Gaussian volume heat source and its peak heat flux decreases with depth, and the model of plasma arc is Gaussian plane heat source. The influence, induced by reaction between laser beam and plasma arc, was mainly studied in the model. Based on the model, the temperature distribution of 2 mm 1420 Al-Li alloy plate was obtained by FEM computation for laser-plasma arc hybrid welding in different distances of two heat sources. The hybrid welding experiments were conducted and show that the simulation results are well agreed with the experimental results. The result proves that the heat transfer model is more close to physical reality. This paper is instructive to research on heat transfer and process about laser-plasma arc hybrid welding.

Key words: laser-plasma arc hybrid welding; finite element method; numerical simulation; Al-Li alloy

Chromium Carbide in situ synthesis by vacuum electron beam LU Fenggui, LU Binfeng, TANG Xinghua, YAO Shun (Welding Engineering Institute, Shanghai Jiaotong University, Shanghai 200030, China). p34—36

Abstract: High hardness composite chromium carbide was successfully produced by in situ synthesis technology, which make it possible to prepare high temperature wear resistance alloy. Chemical reaction among Cr, Fe and C powder which were mixed and laid on the metal surface occurred through vacuum electron beam rotary scanning heating. The resultant of reaction at the metal was identified as Cr_7C_3 composite by X-ray diffraction. And microstructure of composite shows that there is chromium carbide congregated at the metal surface. The mechanical properties show that surface hardness is higher than that of base metal because of chromium carbide. In situ synthesis technology was proved to be a good way to realize metal surface modification.

Key words: vacuum electron beam; in situ synthesis; chromium carbide